FINITE DEFORMATION ANALYSIS OF CYCLIC ELASTOPLASTIC CRACK-TIP FIELDS IN A STRAIN HARDENING MATERIAL

J. Toribio and V. Kharin
Department of Materials Engineering, University of Salamanca
E.P.S., Campus Viriato, Avda. Requejo 33, 49022 Zamora, Spain
Tel: (34-980) 54 50 00; Fax: (34-980) 54 50 02, E-mail: toribio@usal.es

Abstract

Finite-element large deformation analysis of the cracked strain-hardening elastoplastic solid under cyclic loading was performed. Only moderate quantitative changes, but not essential distinctions, were found in the near tip stress fields, if compared with the perfectly-plastic material. On the other hand, with regard to deformations, strain-hardening constitutive behaviour permits the formation of the localised slip bands in the fatigue crack tip. This affects the strain field shape and the rates of plastic strain accumulation in certain locations. The implications of the simulation results for criteria of fatigue crack growth are discussed focusing on the role of loading regime (amplitude and overloads) on crack propagation rate.

Introduction

Analyses of the fine peculiarities of the crack tip stress and deformation fields are essential for understanding of crack propagation phenomena and for development of the predictive tools by means of relating relevant stress-strain characteristics to microscopical rupture mechanisms. Many high-resolution studies of the crack tip fields have been performed (e.g., McMeeking [1], Needleman and Tvergaard [2], Gortemaker *et al* [3], Toribio and Kharin [4]) taking into account physical (plasticity) and geometrical (large deformations) nonlinearities essential for realistic implications for fracture. However, the majority of them are confined to monotonic loading whereas a quite limited data have been generated for fatigue of real material [3] dealing mainly with the idealised perfectly-plastic solid [4].

This contribution focuses on the effect of the strain-hardening constitutive behaviour of a material on the near-tip situation under cyclic loading to provide a more realistic insight about fatigue cracking. Finite deformation simulations of the crack tip fields in the strain-hardening elastoplastic material are presented for a straight plane-strain crack subjected to mode I (opening) cyclic loading under small scale yielding. This presumes that nonlinear material behaviour is localised in a small near tip domain which allows the use of the linear elastic fracture mechanics tool — the stress intensity factor K — as the controlling parameter of the near tip situation irrespective of particular geometry of cracked solid and applied load.

Analysis procedure

As a model, the rate-independent strain-hardening elastoplastic material with von Mises yield surface was considered. Combined isotropic-to-kinematic hardening rule was used which captures the effect of gradual transition towards a stable alternating plastic flow in simple fatigue tests (Suresh [5]). The characteristics of the material corresponded to the experimental data for a high-strength steel (Toribio and Lancha [6]) as follows: Young modulus E = 195 GPa, Poisson ratio μ = 0.3, tensile initial yield stress σ_Y = 1500 MPa, the monotonic load stress-strain curve of the steel is approximated by the Ramberg-Osgood equation which gives the equivalent strain ε_{eq} (plastic component is considered) in terms of the equivalent stress σ_{eq} as $\varepsilon_{eq} = (\sigma_{eq}/P)^n$, where n = 17 and P = 2160 MPa. The double-edge-cracked panel under remote tension was considered with other modelling peculiarities mostly the same as described elsewhere [4].

The nonlinear finite-element code MARC [7] was employed with updated Lagrangian formulation. Calculations were performed for up to ten zero-to-tension load cycles. To avoid premature degeneration of the finite-element mesh and to allow completion of several load reversals in simulations, the near tip mesh and the load stepping procedure in the incremental elastoplastic solution had to be finer than those in similar studies of monotonic loading or a perfectly-plastic material [1-4]. The optimum mesh of 2189 four-node quadrilaterals with 2284 nodes was chosen, the average size of the smallest elements next to the tip being $0.02b_0$.

On the basis of the experiments with the prototype steel [6], the following zero-to-tension fatigue regimes were simulated in relation to the fracture toughness of the steel K_{IC} = 84 $MPam^{1/2}$:

(I) $K_{max} = 0.6K_{IC}$;
(II) $K_{max} = 0.8K_{IC}$;
(III) $K_{max} = 0.6K_{IC}$, overload $K_{ov} = 0.85K_{IC}$ in the 4th cycle

with K_{min} = 0 in all of them, where K_{max} and K_{min} are respectively the maximum and minimum K-levels at constant amplitude cycling, and K_{ov} corresponds to an overload peak. Patterns of applied load vs. time t were sinusoidal in all cases.

Results

Cyclic crack tip fields in the strain-hardening solid display a certain affinity with the behaviour of the perfectly-plastic material, cf. [4]. The crack tip profile evolves with load cycling in a similar manner for all simulated loading regimes. At the initial phase spanning several cycles, the tip shape remains smoothly rounded, like observed earlier in a perfectly-plastic solid [4]. However, with further cycling, substantial distinctions arise. The rounded apex of the tip becomes flattened out and the tip transforms towards a cornered shape, Fig. 1. The higher the previously applied loads, the lower the number of cycles N required to start cornering. Similar phenomenon of the vertex formation on the tip contour (strain localisation) was found in monotonic load calculations for strain-hardening elastoplastic material with a corner (non-Mises) flow theory [2].

With regard to the near tip stress fields, minor quantitative, but not substantial qualitative, distinctions can be found, e.g., comparing the stress distribution pictures and stress-time patterns (see Fig. 2, in this paper the odd times $t = 2N - 1$ correspond to the load maxima and the even ones $t = 2N$ to the minima in the N-th cycle), with analogous data for a perfectly plastic material [4]. The near tip stresses follow along the nearly stable cyclic trajectories with no substantial dependence on the cycle number N. The extrema of the stress values alternation do not vary appreciably with K_{max}, nor they are significantly affected by the overload cycle (Fig. 2).

In contrast to the perfectly-plastic model where the accumulation of strains proceeds rather homogeneously along the round tip contour with the only smooth maximum at the tip apex [4], strain hardening gives rise to strain concentration vertices on the tip profile out of the crack plane. It may be noted in Fig. 1 and is confirmed in Fig. 3 where development of intense shear bands from the corners on the tip contour is evident. The point in the crack plane where one of these bands intersects with its symmetric counterpart is also the location of a strain accumulation peak. The wedge-shaped region near the tip apex between these two bands undergoes relatively little deformation after the bands formation.

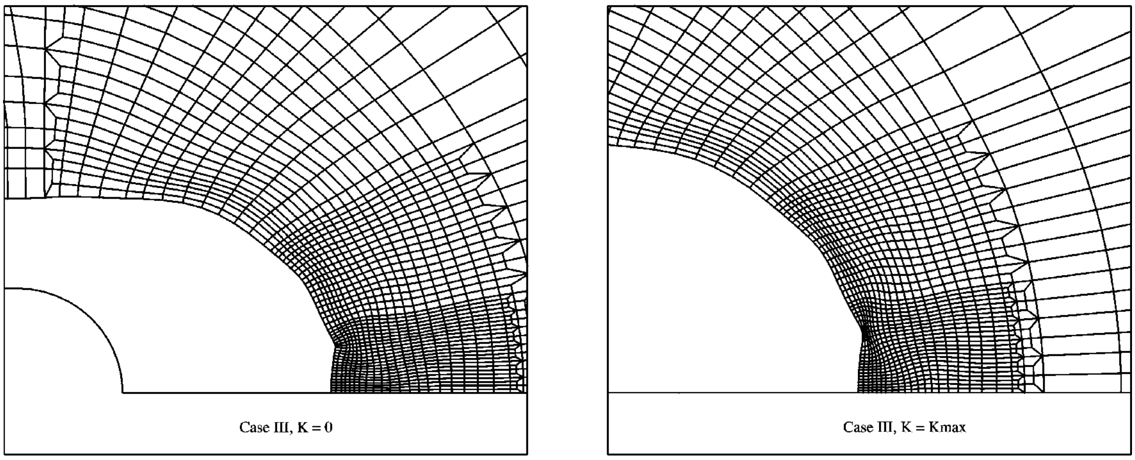

FIGURE 1. Crack tip deformations at different stages of load case III: (a) at t = 12 (K = 0); (b) at t = 13 ($K = K_{max}$); both pictures are in the same scale, the undeformed crack tip of the initial height (twice the radius) of 5 μm is shown in the bottom left corner of the first one.

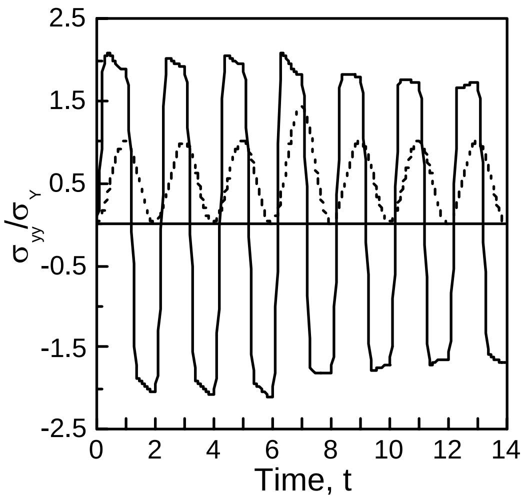

FIGURE 2. Typical pattern of stress evolution near the crack tip at sine-shape applied load pattern (shown for reference in arbitrary units by the dotted line) at loading regime III.

The total (accumulated) equivalent plastic strain along the loading path, $\varepsilon_{tot} = \int \varepsilon_{eq} dt$, which supposedly controls fatigue damage accumulation [5], increases with fairly constant cyclic rates $d\varepsilon_{tot}/dN$ everywhere in the crack tip zone provided strain localisation has not started yet, as in the load case I and initial stage of the loading regime II (Fig. 4). In the later stage of the loading regime II, after shear band initiation at $t \approx 6$, plastic strain accumulation accelerates sharply within the bands, decelerates in the interior of the wedge-shaped zone between the bands (similar to one shown in Fig. 3), and maintains apparently constant rate outside. The accumulation rates in the course of constant amplitude cycling are higher for greater values of K_{max}. In the regime with an overload, the strain accumulation everywhere in the close vicinity of the tip after load peak proceeds with about the same rates $d\varepsilon_{tot}/dN$ as before, provided shear bands have not developed yet, as demonstrated by the curves 1 and 2 in Fig. 5 for $t \leq 10$. After they appear, accumulation of strain accelerates within the band and nearly finishes in the wedge-shape domain at the tip apex between the slip bands, in the same manner as under constant amplitude loading (curves 1 and 2 in Figs. 5 and 4 respectively). However, the instantaneous values of strain $\varepsilon_{eq}(t)$, which have been oscillating in a ratcheting manner, stop climbing throughout the whole process zone after overload (Fig. 5, curves 3 and 4).

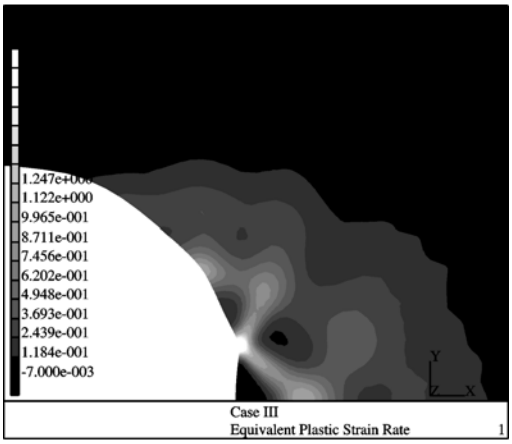

FIGURE 3. Distribution of the equivalent plastic strain rate $d\varepsilon_{eq}/dt$ (arbitrary units) at approaching K_{max} in the loading case III.

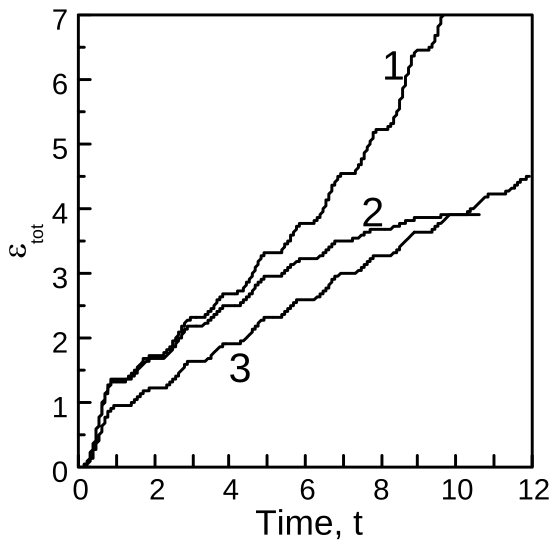

FIGURE 4. Accumulation of equivalent plastic strain near the crack tip under constant amplitude loading regimes I and II at material points located at about the same distance from the crack tip contour: in the shear band and in the wedge-shaped zone between the bands (namely, at the tip apex) in load case II [(1) and (2), respectively]; (3) in the tip apex when shear bands do not arise in load case I.

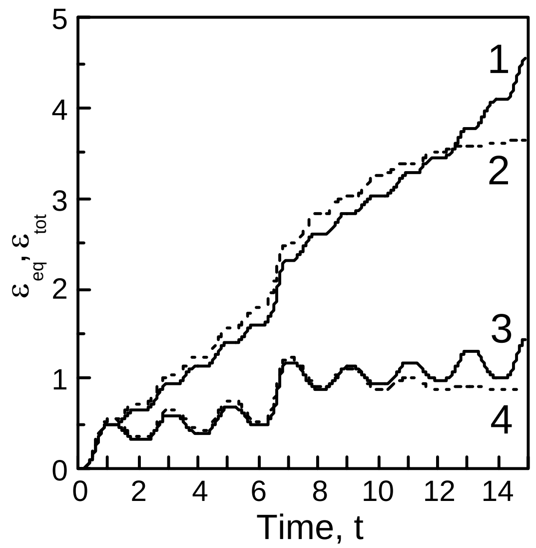

FIGURE 5. Strain accumulation ε_{tot} (curves 1 and 2) and evolution of plastic strain ε_{eq} (curves 3 and 4) near the crack tip at material points located at about the same distance from the crack tip contour during fatigue with an overload peak at t = 7 (load case III) in the shear band (solid lines) and in the wedge-shaped zone between the bands (dashed curves).

Discussion

In the light of the reported results, certain implications may be derived with regard to the criteria of fatigue crack growth. These criteria are usually derived associating local rupture event with some critical condition in terms of local stress, strain, or both them as governing factors of fatigue degradation of material. Numerical modelling shows that the stress fields in the supposed fracture process zone are nearly insensitive to the fatigue loading parameters (the amplitude K_{max} and overload level K_{ov}) at least in a certain range of their variation. In all simulated regimes, stresses oscillated between nearly equal tension-compression limits. This contrasts with rather general experimental trends of increase of the fatigue crack growth rates with K_{max} and retardation of the constant amplitude fatigue crack propagation after an overload peak [5].

Total plastic strain ε_{tot} as a candidate key parameter of the local failure criterion manifests better correspondence with experimental data about the role of K_{max}: experimental crack growth and calculated strain accumulation both accelerate with the load amplitude increase. However, this affinity fails with regard to the effect of a single overload on fatigue.

Comparing the accumulation of strain, ε_{tot}, with its evolution, $\varepsilon_{eq}(t)$, reveals better parallelism of the latter with crack growth data concerning the role of both load amplitude and overloads. Although $\varepsilon_{eq}(t)$ oscillates, its maxima increase with cycle number faster at higher K_{max}, and this increase is arrested by an overload peak (Fig. 5). Then critical strain criterion of local rupture seems to be promising to predict fatigue crack extension. However, taking into account that experimental crack growth is delayed by an overload peak, but not finished, a combined critical condition may be required supposing that the limit level of the instantaneous strain ε_{eq} at rupture would be a function of the accumulated strain ε_{tot} to represent increase of material degradation, probably up to a certain maximum saturated level.

Conclusion

High-resolution large deformation finite-element analysis of a stationary plane-strain tensile crack in the strain-hardening elastoplastic material under various fatigue load patterns reveals good agreement of the calculated characteristics of the plastic strains in the near tip zone with the experimental trends of the variation of the fatigue crack growth rate depending on the applied load amplitude and overload peaks. This creates a promising basis for linking stress-strain analysis with micromechanical rupture mechanism and prediction of the fatigue crack extension in structural materials.

Acknowledgements

The authors wish to thank the financial support of this work by the following institutions: Spanish Ministry for Scientific and Technological Research MCYT-FEDER (Grant MAT2002-01831), FEDER-INTERREG III (Grant RTCT-B-Z), Junta de Castilla y León (JCYL; Grant SA078/04) and Spanish Foundation “Memoria de D. Samuel Solórzano Barruso”. In addition, the authors wish to thank EMESA TREFILERIA S.A (La Coruña, Spain) for providing the steels used in the experimental programme.

References

1. McMeeking, R.M., *J. Mech. Phys. Solids*, vol. **25**, 357–38, 1977.
2. Needleman, A. and Tvergaard, V., *ASTM STP 803*, vol. **I**, I-80–I-115, 1983.
3. Gortemaker, P.C.M., de Pater, C. and Spiering, R.M.E.J., *Proc. 5th Int. Conf. Fracture*, edited by D. Francois, Pergamon Press, Oxford, 1981, 151–160.
4. Toribio, J. and Kharin, V., *Fracture From Defects. Proc. 12th European Conference on Fracture*, edited by M.W. Brown *et al*., EMAS, West Midlands, 1998, 1059–1064.
5. Suresh, S., *Fatigue of Materials*, Cambridge University Press, 1991.
6. Toribio, J. and Lancha, A.M., *Mater. and Struct*., vol. **26**, 30–37, 1993.
7. MARC User Information, Marc Analysis Research Corp., Palo Alto, 1994.